Fault-Resilient Direct Torque and Power Control Strategy for Back-to-Back Converters in Direct-Drive PMSG Wind Energy Conversion Systems

GUDISE HARITHA[1], S. Anusha[2], M. Sirisha[3]
[1]Post Graduate Student, JNTUA College of Engineering, Anantapuram
[2]Assistant Professor (Adhoc), JNTUA College of Engineering, Anantapuram
[3]Assistant Professor (Adhoc), JNTUA College of Engineering, Anantapuram
[1]harithalucky13@gmail.com, [2]sankranthi.anusha2425@gmail.com, [3]shirishamesa1031@gmail.com

Abstract:

Fault tolerance is considered crucial in wind turbines to increase reliability and availability. This article describes a fault-tolerant permanent magnet with direct drive and innovative direct control synchronous generator PMSM techniques that can handle high-power semiconductors OPEN-CIRCUIT failure in back-to-back trans missions. The fault-tolerance system consists of five legs. A converter with an interconnected leg linked to an alternator phase, a converter with a shared leg connected to an alternator phase, and a converter with an Alternating Current Triode to its proper grid phase. The development of DTC and DPC procedures for MSC and GSC is the primary contribution of this study. A reliable failure diagnostics method is also provided, providing the information required to immediately activate fault-tolerant remedial measures without the usage of additional sensors. To demonstrate the effectiveness of the proposed fault-tolerant PERMANENT MAGNET SYNCHRONOUS GENERATORS drive, simulation and experimental data are presented.

Term index: Fault-tolerant back-to-back converters, GRID SIDE(GS) converter, machine side(MS) (DTC), (DPC), power switch open-circuit failures, PMSM, and wind turbine systems.

Introduction:

As wind energy begins to have a substantial impact on the power grid, efficient, dependable, and renewable power transformation at low-cost technologies is required. Wind energy with drive systems based on (PMSG) with full-scale Back-Back converters, with (DTC) and (DPC) for connection between the alternator and the matrix management, are a promising technology. Despite the fact that wind turbine technology has advanced substantially in recent years, its dependability and availability remain lower than predicted [1], according to industry statistics [2], Power transistors, on the other hand, are the most common source of catastrophic malfunctions. [2], [3]. It is critical to design fault-tolerant converters that can retain operating when an unanticipated power switch defect occurs, in order to improve reliability and availability. Because SC shielding is a regular feature for industrial drives, this article considers power switch open-circuit problems.

Various OPEN CIRCUIT fault detection methods with minimal computing needs and no extra hardware. Diagnostic techniques new adaptive limits for numerous power switch OPEN CIRCUIT issues were recently devised in [8], [10], greatly increasing the resilience of these algorithms.

Furthermore, an extra voltage sensor is necessary to reduce voltage fluctuations, increasing the drive's complexity and expense. A four-leg converter architecture was presented in [18], with failures in two distinct converters Aside from the direct current bus midway contact concerns, the architecture necessitates the use of six Triode for Alternating Currents, which adds to the system's complexity and expense. Possibly (FLC-SL) scheme has presented to alleviate difficulties associated with the dc bus midway connection, through coupling the motor components to the network phases that they belong to [19]-[22]. Comparable topologies linking two similar motor phases were proposed in [23]-[30]. When compared to SLC schemes, the performance of these topologies is lower, and more legs sustaining functioning. This architecture, however, necessitates the use of a transformer at the network coupled point, and the linked arms must have constructed through four-fold higher rated current. 2 machines are linked with its ground points in [32], resulting in a threefold increase in phase currents. Such a design enables the system to run within restricted moving the operational life to post-fault management without oversizing component ratings due to a drop in converter voltage capacity or an increase in current.

Modifying the typical PWM modulation allows for separate control of both converters. As a consequence, each converter's output voltage is simultaneously limited to fifty percent of Direct current output voltage, and varied among converters arms shifting frequency may be achieved. Furthermore, proportional-integral current controllers and understanding of the system model/parameters are required for these control strategies. Hysteresis current controllers are used in [17], [27], and [31] to achieve straightforward implementation, rapid response, and parameter independence. [18], [19], [28], and [30] all suggested model predictive control approaches. Fast control dynamics and the flexibility to integrate various restrictions in a specified cost function are the key features of these control systems. These strategies, unlike simple hysteresis control, need knowledge of motor models and parameters, as well as a significant amount of online computation work owing to cost function limits.

DTC, DPC schemes were used to connect the PERMANENT MAGNET SYNCHRONOUS GENERATORS phases to their appropriate grid phases through 3 extra Triode for Alternating Currents, eliminating the problems associated with the dc-link midpoint connection. The proposed DTC and DPC approaches use 2 new shifting table to provide 6 active voltage vectors and 2 ZVV for each converter, additionally improving drive control output. Furthermore, real-time fault diagnosis technique introduced in [8] is used to initiate fault-tolerant remedial actions in this article. Simulation and experimental findings are used to assess and confirm the performance of the proposed fault tolerant PERMANENT MAGNET SYNCHRONOUS GENERATORS drive.

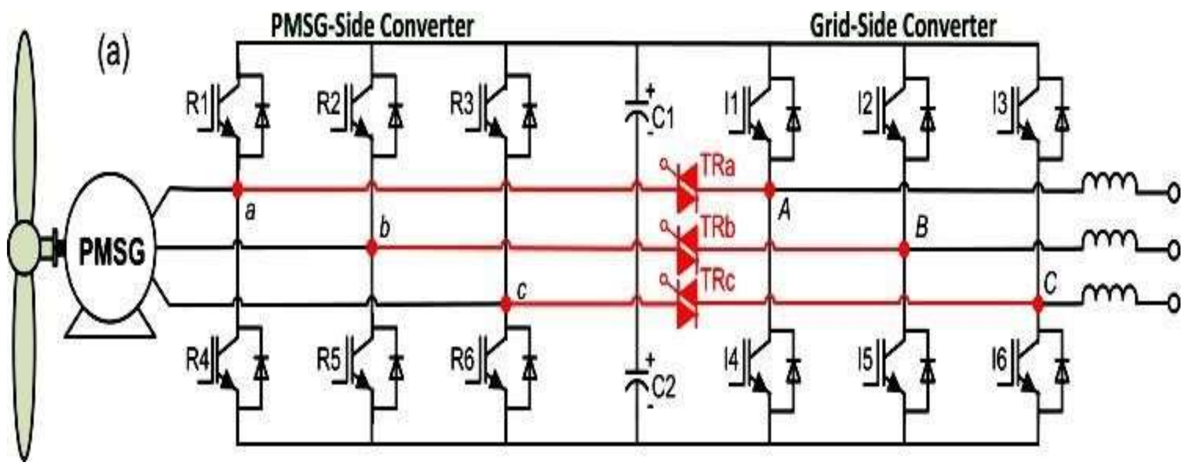

II. FAULT-TOLERANT CONVERTER TOPOLOGY

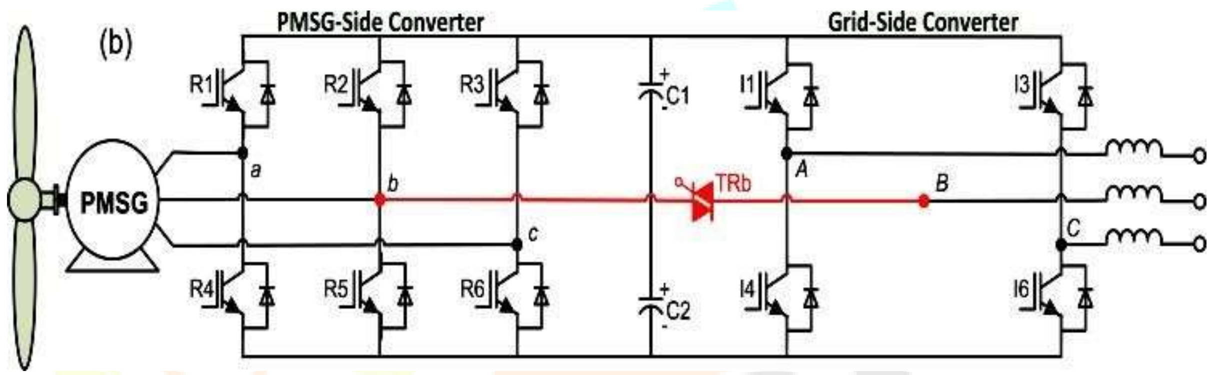

Fig. 1. Fault-tolerant converter topology: (a) under healthy operating conditions, (b) after OPEN CIRCUIT fault occurrences in leg "B" (I2 or I5).

The suggested fault-tolerant converters architecture is based on a back-to-back converter with three extra Triode for Alternating Currents connecting the generator phases with its respective grid phases and remaining open during standard operating circumstances. This design provides for continuing drive operation in the event of an open circuit failure, with one common arm linked to the grid and machine phases via the Triode for Alternating Current. Consider the following example of an O-C failure in the GS CONVERTER Insulated Gate Bipolar Transistor I2 or I5: The afflicted leg will be isolated when the problem is detected by eliminating the gate command signals to Insulated Gate Bipolar I2 and I5. By triggering on the Triode for Alternating Current TRb, the grid-phase B will be coupled to its equivalent machine-phase b, changing the converter topology from a typical SLC to an FLC-SL. In the instance of an OPEN CIRCUIT failure in INSULATED-GATE BIPOLAR TRANSISTOR R2 or R5 of the machine- side converter, triggering on the Triode for Alternating Current TRb connects phases b and B. The incorporated Triode for Alternating Current is designed to rearrange the power converter topology's circuit, ensuring current flow between both the PERMANENT MAGNET SYNCHRONOUS GENERATORS and network phases.

III. STRATEGIES FOR CONVERTER DIRECT MANAGEMENT

Specific alterations to back-to-back converter's post-fault regulating scheme are designed to change them with the relevant converter architecture and drive management system

A. Model of the converter

In a back-to-back architecture, power converters are linked. As illustrated in Fig. 1, every converter is considered as a standard VSI with 6 INSULATED-GATE BIPOLAR TRANSISTORs and associated antiparallel diodes (a). The voltage space vectors for MS CONVERTERS are specified by

$$V_{s1} = \frac{2}{3}\left(u_{an} + u_{bn}e^{j2\pi/3} + u_{cn}e^{j4\pi/3}\right) = u_{s\alpha} + ju_{s\beta} \quad (1)$$

The space voltage vector has a maximum amplitude of□□□/√3. The voltages □□□ (k = a, b, c) may be determined by

the equation of the □□0 phase-to-zero and □□0 neutral-to-zero voltages.

$$u_{an} = u_{a0} - u_{n0},\ u_{bn} = u_{b0} - u_{n0},\ u_{cn} = u_{c0} - u_{n0} \quad (2)$$

where

$$u_{n0} = \frac{u_{a0} + u_{b0} + u_{c0}}{3}$$

in turn, the voltages uk0 are defined by the states of switching:

$$u_{a0} = u_{dc}S_a,\ u_{b0} = u_{dc}S_b,\ u_{c0} = u_{dc}S_c \quad (3)$$

□□(k=a, b, c) denotes the switching states of INSULATED-GATE BIPOLAR TRANSISTORs R1, R2 and R3 in phases a, b, and c, respectively. When (3) is substituted for (2) and (2) for (1), the connection is between the output voltages of the converter and the switching voltages.

$$\begin{pmatrix} u_{an} \\ u_{bn} \\ u_{cn} \end{pmatrix} = \frac{u_{dc}}{3}\begin{pmatrix} 2 & -1 & -1 \\ -1 & 2 & -1 \\ -1 & -1 & 2 \end{pmatrix}\begin{pmatrix} S_a \\ S_b \\ S_c \end{pmatrix} \quad (4)$$

B. Direct torque controls technique of the 3-phase machine side converter

Both electromagnetic torque and stator flux are regulated directly and individually in the Direct Torque Control approach [33]. They may be calculated using a surface-mounted PERMANENT MAGNET SYNCHRONOUS GENERATORS mathematical model in a stationary reference frame.

$$\begin{cases} u_{s\alpha} = R_s i_{s\alpha} + \frac{d}{dt}\psi_{s\alpha} \\ u_{s\beta} = R_s i_{s\beta} + \frac{d}{dt}\psi_{s\beta} \end{cases} \quad (5)$$

$$\begin{cases} \psi_{s\alpha} = L_d i_{s\alpha} + \psi_{PM}\cos\theta \\ \psi_{s\beta} = L_q i_{s\beta} + \psi_{PM}\cos\theta \end{cases} \quad (6)$$

$$T_e = \frac{3}{2}\frac{p\left|\psi_s\right|\psi_{PM}}{L_d}\sin\delta = \frac{3}{2}p\left(\psi_{s\alpha}i_{s\beta} - \psi_{s\beta}i_{s\alpha}\right) \quad (7)$$

The current model-based technique may be used to estimate the stator flow (6). The electromagnetic torque, on the other hand, is regulated by adjusting the stator flux amplitude and the load angle between the stator and rotor flux vectors (7).

This is performed by selecting the appropriate voltage space vectors, that enables the magnitude and path of the stator flux to be modified according to requirements. (5). The space vector plane is separated into six sectors to make picking these vectors easier. First, a set reference flux is enforced, while the speed controller generates the electromagnetic torque reference. Then, using two-level hysteresis controllers, the stator flux and electromagnetic torque errors are limited, with hysteresis bands B□s and BTe defined, respectively. The hysteresis controller outputs d
□s and dTe govern whether the flux linkage and torque should increase (+) or decrease (-).

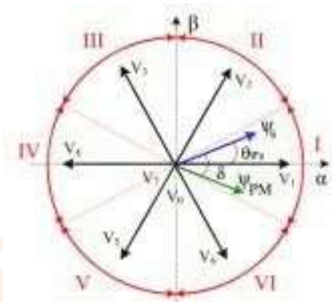

Fig. 2 Sector classification as per the stator flux vector and voltage vectors produced by the MACHINE-SIDE CONVERTER

TABLE I: DTC SWITCHING TABLE FOR THE MSC

$d\Psi_s$	dT_e	Sector I	Sector II	Sector III	Sector IV	Sector V	Sector VI
+	+	V2 (110)	V3 (010)	V4 (011)	V5 (001)	V6 (101)	V1 (100)
	-	V6 (101)	V1 (100)	V2 (110)	V3 (010)	V4 (011)	V5 (001)
-	+	V3 (010)	V4 (011)	V5 (001)	V6 (101)	V1 (100)	V2 (110)
	-	V5 (001)	V6 (101)	V1 (100)	V2 (110)	V3 (010)	V4 (011)

C. Direct power control of the 3-phase GS CONVERTER

The Direct Power Control approach [34] controls active and reactive powers directly and separately, similar to the Direct Torque Control technique, by picking the best voltage vector in a shifting block. The instantaneous power derivatives technique introduced is used in the study to create an upgraded switching table.

The network-current and voltage dynamics may be used to determine the instantaneous power derivatives. The grid voltages in the stationary reference frame are as follows:

$$\begin{cases} u_{g\alpha} = -R_f i_{g\alpha} - L_f \dfrac{di_{g\alpha}}{dt} + u_{c\alpha} = U_g \sin(\omega_g t) \\ u_{g\beta} = -R_f i_{g\beta} - L_f \dfrac{di_{g\beta}}{dt} + u_{c\beta} = -U_g \cos(\omega_g t) \end{cases} \quad (8)$$

The instantaneous active and reactive powers of the grid are defined as follows:

$$\begin{cases} p_g = u_{g\alpha} i_{g\alpha} + u_{g\beta} i_{g\beta} \\ q_g = u_{g\beta} i_{g\alpha} - u_{g\alpha} i_{g\beta} \end{cases} \quad (9)$$

$$\begin{cases} \frac{dp_g}{dt} = u_{g\alpha} \frac{di_{g\alpha}}{dt} + i_{g\alpha} \frac{du_{g\alpha}}{dt} + u_{g\beta} \frac{di_{g\beta}}{dt} + i_{g\beta} \frac{du_{g\beta}}{dt} \\ \frac{dq_g}{dt} = u_{g\beta} \frac{di_{g\alpha}}{dt} + i_{g\alpha} \frac{du_{g\beta}}{dt} - u_{g\alpha} \frac{di_{g\beta}}{dt} - i_{g\beta} \frac{du_{g\alpha}}{dt} \end{cases} \quad (10)$$

As a result, we have the instantaneous power derivatives.

where you may get the instantaneous current fluctuations from (8)

$$\begin{cases} \frac{di_{g\alpha}}{dt} = \frac{u_{c\alpha} - u_{g\alpha} - R_f i_{g\alpha}}{L_f} \\ \frac{di_{g\beta}}{dt} = \frac{u_{c\beta} - u_{g\beta} - R_f i_{g\beta}}{L_f} \end{cases} \quad (11)$$

and the network voltage fluctuations were

$$\begin{cases} \frac{du_{g\alpha}}{dt} = \omega_g U_g \cos(\omega_g t) = -\omega_g u_{g\beta} \\ \frac{du_{g\beta}}{dt} = \omega_g U_g \sin(\omega_g t) = \omega_g u_{g\alpha} \end{cases} \quad (12)$$

The instantaneous active and reactive power derivatives may written by substituting (11) and (12) in (10), disregarding Rf, and treating both pg and qg as null (starting condition).

$$\begin{cases} \frac{dp_g}{dt} = -\frac{1}{L_f}\left(u_{g\alpha}^2 + u_{g\beta}^2 - u_{g\alpha} u_{c\alpha} - u_{g\beta} u_{c\beta}\right) \\ \frac{dq_g}{dt} = \frac{1}{L_f}\left(u_{g\beta} u_{c\alpha} - u_{g\alpha} u_{c\beta}\right) \end{cases} \quad (13)$$

The acquired instantaneous reactive and active power changes generated through use of every voltage vector with a instant of the network voltage were displayed in fig.3 by replacing every voltage vector with 3Ø converter could synthesise in 13. Active power reference is generated with dc bus voltage controller in the DIRECT POWER CONTROL approach, and the network UPF is guaranteed through inducing a reference null reactive power. The powers controller are then set up using BP and BQ hysteresis bands, respectively. The dP and dQ outputs of the hysteresis comparator determine whether the reactive and active powers are supposed to increase (+) or decrease (-).

As a result, the switch The instantaneous power derivatives shown in Fig. 3 are used to create Table II. It's vital to note that, in the case of Direct Torque Control, the space vector plane is split into six sectors based on the grid voltage vector angle, as shown in Fig 2. The switching Table II, on the other hand, is designed to pick the voltage

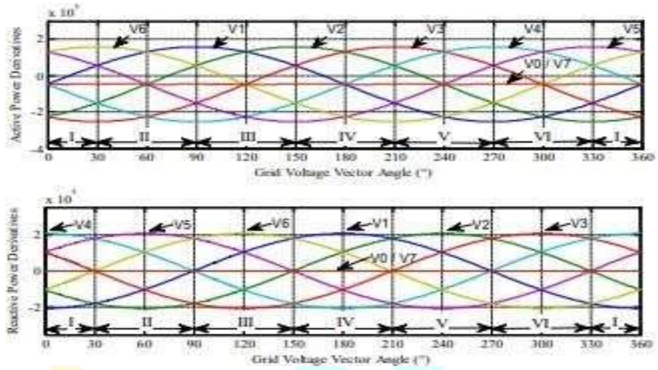

vector that causes the greatest fluctuation in pg, based on the grid voltage vector angle.

Fig. 3: GS CONVERTER-imposed differentiated instantaneous reactive and active power

TABLE II: DPC SWITCHING TABLE FOR THE GSC

dP	dQ	Sector I	II	III	IV	V	VI
+	+	V5 (001)	V6 (101)	V1 (100)	V2 (110)	V3 (010)	V4 (011)
	-	V6 (101)	V1 (100)	V2 (110)	V3 (010)	V4 (011)	V5 (001)
-	+	V3 (010)	V4 (011)	V5 (001)	V6 (101)	V1 (100)	V2 (110)
	-	V2 (110)	V3 (010)	V4 (011)	V5 (001)	V6 (101)	V1 (100)

D. DCT of Five Leg Converter with Shared Leg

Figure 4 depicts the suggested faults-tolerance regulating techniques. Switching occurs during converter post-fault operation.The post-fault regulation technique is adapted to latest converter system using Tables I and II. The accurate limits of the stator flux error * s ss and the accurate limits of reactive power error * Qqq g g were related, with the goal of assigning control priority to one of the converters and achieving individual regulation.

$$priority = \begin{cases} P, Q & if \ |\Delta\psi_s| < \lambda|\Delta Q| \ and \ |\Delta T_e| < T_{th} \\ \psi_s, T_e & otherwise \end{cases} \quad (14)$$

The choice of Tth is critical since this have a significant influence over drive's output below post-fault situations. While deciding on, the stator flux and reactive power errors in normal condition are taken into account. Because stator flux and reactive power are sometimes of different degrees, its errors are not all equivalent.

As a result, the value of is chosen to compensate for the fact that the stator flux and reactive power mistakes are of different natures. Under typical conditions, the electromotive force is managed in a rather manner that the torque variation is maintained only within prescribed hysteresis band BTe.The torque error exceeds the required band owing to the ZVV provided to the MS CONVERTER during post-fault operation, resulting in unwanted electromagnetic torque oscillations. As a consequence, the torque hysteresis band BTe's quantity for the threshold T (th) reduces the ZVV given for MS CONVERTER., resulting in a smooth torque development.

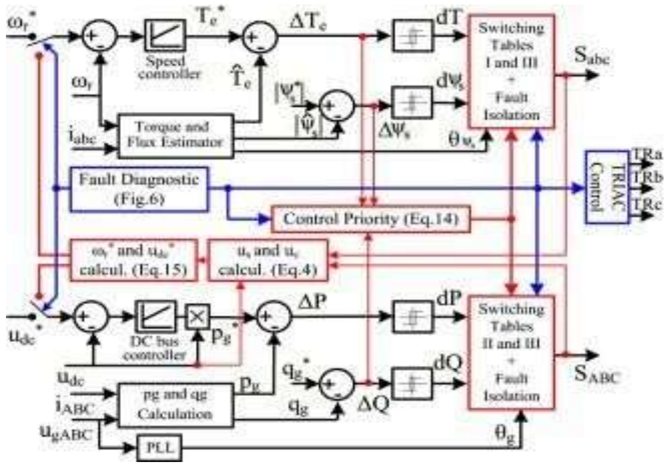

Fig. 4 The back-to-back converter with reprogrammable DTC.

It's worth noting that the values of and □□h have been kept constant to provide the highest possible performance while also simplifying the control. Table III is used to create the switching tables for the DTC, DPC. Given arm b of MS CONVERTER is the linked arm if switching states and torque error are smaller that of reactive power and □□h simultaniously, control of the GS CONVERTER's instantaneous powers is given precedence.

TABLE III: VOLTAGE VECTORS OF THE FLC-SL

Shared leg		Priority	Feasible voltage vectors of	
Leg	State		GSC	MSC
a or A	1	P,Q	V1,V2,V6	V1,V2,V6,V7
		Ψ_s,T_e	V1,V2,V6,V7	V1,V2,V6
	0	P,Q	V3,V4,V5	V3,V4,V5,V0
		Ψ_s,T_e	V3,V4,V5,V0	V3,V4,V5
b or B	1	P,Q	V2,V3,V4	V2,V3,V4,V7
		Ψ_s,T_e	V2,V3,V4,V7	V2,V3,V4
	0	P,Q	V1,V5,V6	V1,V5,V6,V0
		Ψ_s,T_e	V1,V5,V6,V0	V1,V5,V6
c or C	1	P,Q	V4,V5,V6	V4,V5,V6,V7
		Ψ_s,T_e	V4,V5,V6,V7	V4,V5,V6
	0	P,Q	V1,V2,V3	V1,V2,V3,V0
		Ψ_s,T_e	V1,V2,V3,V0	V1,V2,V3

IV. ASPECTS FOR SYSTEMS INTEGRATION AND POST-FAULT WORKING CONFINES

A. Performance of converter

During post fault period, converter works at rated power necessitates over sizing the output ratings of the power converter. Its working in dreaded method, on other hand, permits the drive for function within restricted range through or lacking over sizing converters' component limits. Due to fault-tolerant converter topology's lower voltage capability and the constant grid voltage, increasing the dc-link voltage and/or lowering the alternator speediness were2 options accessible to keep converters operating in linear variation area and avoid higher rotation and current deviation. The linear variation ... ed leg will give by

$$u_s + u_c \le \frac{u_{dc}}{\sqrt{3}} \quad (15)$$

.

As a result, the extreme speediness is restricted through MS CONVERTER voltage's maximum amplitude, which is given by

$$u_{s,max} = \frac{1}{\sqrt{3}} u_{dc,max} - u_{c,max} \quad (16)$$

As a result, after performing the us and u_C computations (4).

Table IV compares the fault tolerant converter architecture under consideration with the various non-redundant converter topologies appropriate for PERMANENT MAGNET SYNCHRONOUS GENERATORS drives. The esteemed working limits over post fault working is taken into account for a fair comparison. with faults-tolerance windmill, a low rise in the extra hardware need is preferred, since this avoids increasing the system cost and complexity. Because it only takes a small quantity of additional apparatus for achieving faults tolerant, the proposed topology is more cost-effective for wind turbine applications. Instead of the six Triode for Alternating Currents utilised in a back-to-back topology in [18], three are required.

TABLE IV. COMPARISON OF FAULT-TOLERANT CONVERTER TOPOLOGIES

			Standard Converter	Topology in [16]	Topology in [17]	Topology in [18]	Topology in [31]	Proposed Topology
Additional Hardware Requirements			-	3 (TRIAC) 1 (Volt. Sensor)	1 (TRIAC) 1 (Volt. Sensor) 1 (Transf.)	6 (TRIAC) 1 (Volt. Sensor)	1 (TRIAC) 3 (Relay) 1 (Transf.)	3 (TRIAC)
Volt. Capability / u_{dc}			58%	29%	50%	29%	37%	29%
IGBTs	Rating Increase	V	-	100%	15%	100%	58%	100%
		I	-	-	$\sqrt{3}\, I_{Grid}$	-	$3I_{Grid}+I_{PMSG}$	$I_{Grid}+I_{PMSG}$
Capacitors	Rating Increase	V	-	100%	15%	100%	58%	100 %
		I	-	I_{Grid}	$3I_{Grid}$	$I_{Grid}+I_{PMSG}$	-	-

The Triode for Alternating Currents linked with alternator phases for its corresponding network phases, removing need for a interlink with direct current bus average point, which necessitates careful design of the dc bus midpoint [16]-[18]. the capacitors, as well as a voltage sensor with a wider bandwidth. By connecting, the converter's voltage capacity is improved. The linked leg to the transformer neutral is connected through a Triode for Alternating Current. 31st point In order to interface the wind, a transformer is incorporated at the output of a low-voltage back- to-back converter. grid-connected energy conversion system However, because of a significant increase in the spectrum of wind generation for multi-Mega Watts, a 1 low-voltage back-to-back converter is no longer useful. M is quite convenient.

B. Dynamic Load

The utmost difficult challenge in the execution procedure be located to guarantee that there is very little calculation spell interruption thus faults-tolerance regulate output isn't harmed. Consequently, length of time it took to implement the code is also utilized as a criteria.to assess the computational overhead of the suggested direct method advanced model prediction approaches and techniques of control [18], [19], [28]-[30]. Figure 5 depicts the implementation detail in real-time. For the PERMANENT MAGNET SYNCHRONOUS GENERATORS drive with two-level back-to-back converter, the measured regulator and regulator are accepted and employed using MatLab Simulink. Since its easiness, the presented Direct Torque Control, Direct Power Control systems complete encryption execution in a sample time in just 18.04 seconds, which is much less time than the model predictive control presented in [50]. Alternative methods based on Direct Torque Control are newly developed to reduce the execution difficulty of perfect analytical regulator approaches due to low computing needs of direct control techniques. The execution durations of diagnostic and reconfiguration algorithms for the examined fault tolerant control methods. As a result, suggested fault-tolerant control techniques are thought to have a minimal computational load.

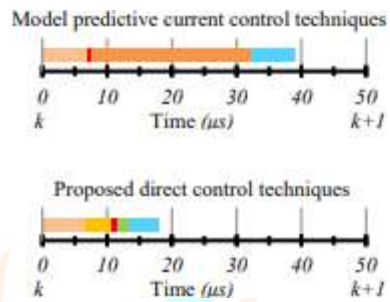

Fig 5 MPCT AND DCT

V. FAULT DIAGNOSTICS

Suggested a fault diagnostics approach for identifying multiple OPEN CIRCUIT failures in PERMANENT MAGNET SYNCHRONOUS GENERATORS drives that did not require the use of any extra sensors. The proposed approach is used in this study to detect an unanticipated OPEN CIRCUIT failure and initiate appropriate corrective actions. To begin, 2 CFFs were determined to every MS CONVERTER and GS CONVERTER phase. The CFFs FFk and FF K (K=a, b, c) are computed using measured and observed MACHINE- SIDE CONVERTER currents, respectively (see Fig. 6). FFj, on the other hand, the form factor estimated through the GS CONVERTER's measured and observed currents, respectively. Adaptive thresholds for FFk and FFj are FF k and FF j, correspondingly. As a result, positive empirically determined constant values s and g are added to FF k and FF j, respectively.0.1 and 0.2 were chosen as the constant values for s and g, respectively. [8] explains the actual technique for selecting all of the constant values and thresholds in further detail. The obtained adaptive thresholds Sk and Sj are bigger than FFk and FFj under healthy operating conditions. j. When and INSULATED-GATE BIPOLAR TRANSISTOR OPEN CIRCUIT error happens, the constant form factor values of FFk/FFj linked to defective phase crosses its corresponding adaptive threshold, indicating that a fault exists in it. It's worth noting to diagnose procedure relies on data from current sensors as well as data from previous sensors. amounts already in the primary control Since The reference voltages are calibrated using direct control techniques. calculated from the pattern of switching (4).

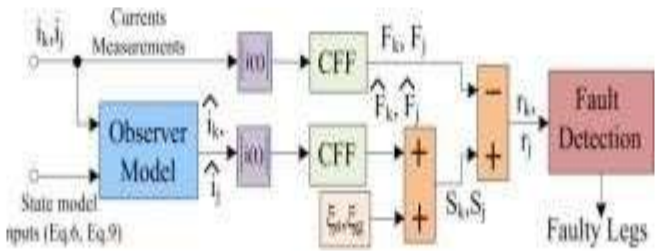

fig 6 Fault detection procedure schematic diagram.

VI. Simulation Outcomes

Simulation in Matlab Simulink environment was used to evaluate the proposed fault-tolerant topology. The PERMANENT MAGNET SYNCHRONOUS GENERATORS drive system has the same construction as the one shown in Fig. 1. (a). The MS CONVERTER and GS CONVERTER, respectively, are subjected to the DTC, DPC tactics. PERMANENT MAGNET SYNCHRONOUS GENERATORS connected to a four-quadrant test bench, two back-to-back Powered POW-R-PAK voltage source converters, Table V displays the PERMANENT MAGNET SYNCHRONOUS GENERATORS parameters. Direct control approaches with the suggested fault-tolerant control are incorporated into the dSPACE digital controller board utilising Matlab Simulink and a sampling time of 50 seconds. all of the findings were obtained with a constant grid phase-to-phase RMS voltage of 50 V and a maximum dc link voltage of 285 V.

TABLE V: PMSG PARAMETERS

Power	P	2.2 kW
Speed	N	1750 rpm
Voltage	V	316 V
Current	I	5.3 A
Torque	T_L	12 N.m
Frequency	f	145.8 Hz
Armature Resistance	R_s	1.72 Ω
Magnet flux linkage	ψ_{PM}	0.244 Wb
d/q-axis inductance	$L_{d/q}$	20.5 mH

BTe and Bs were set to 2% and 1% of the torque and flux rated values, respectively, for the Direct Torque Control. The hysteresis bands BP and BQ, which approximate to 0.002 percent of the PERMANENT MAGNET SYNCHRONOUS GENERATORS rated power, were chosen for the Direct Power Control. As a consequence, 0.055 and 0.24 are the values of and □□h , respectively. 5-ARM converters through connected arm b for MS CONVERTER is examined in Figs. 8 and 9.

The network reactive power deviation is below the PERMANENT MAGNET SYNCHRONOUS GENERATORS stator flux error when constant values of 2/3 and □□h are applied (14) As a result, the PERMANENT MAGNET SYNCHRONOUS GENERATORS currents have more sinusoidal waveforms, but the network output currents have a large deviation, consequential in large fluctuating instantaneous powers. The excellent agreement between modelling can be shown in Figs. 9 (a).

As a result, the MS CONVERTER and GS CONVERTER's independent control condition is confirmed. The suggested control technique may also form sinusoidal apparatus and network currents, as can be observed. Equally EMT as well as stator flux may be regulated using Direct Torque Control in conjunction by swapping Tables III and I, resulting in correct speed monitoring and a balanced three-phase PERMANENT MAGNET SYNCHRONOUS GENERATORS current system

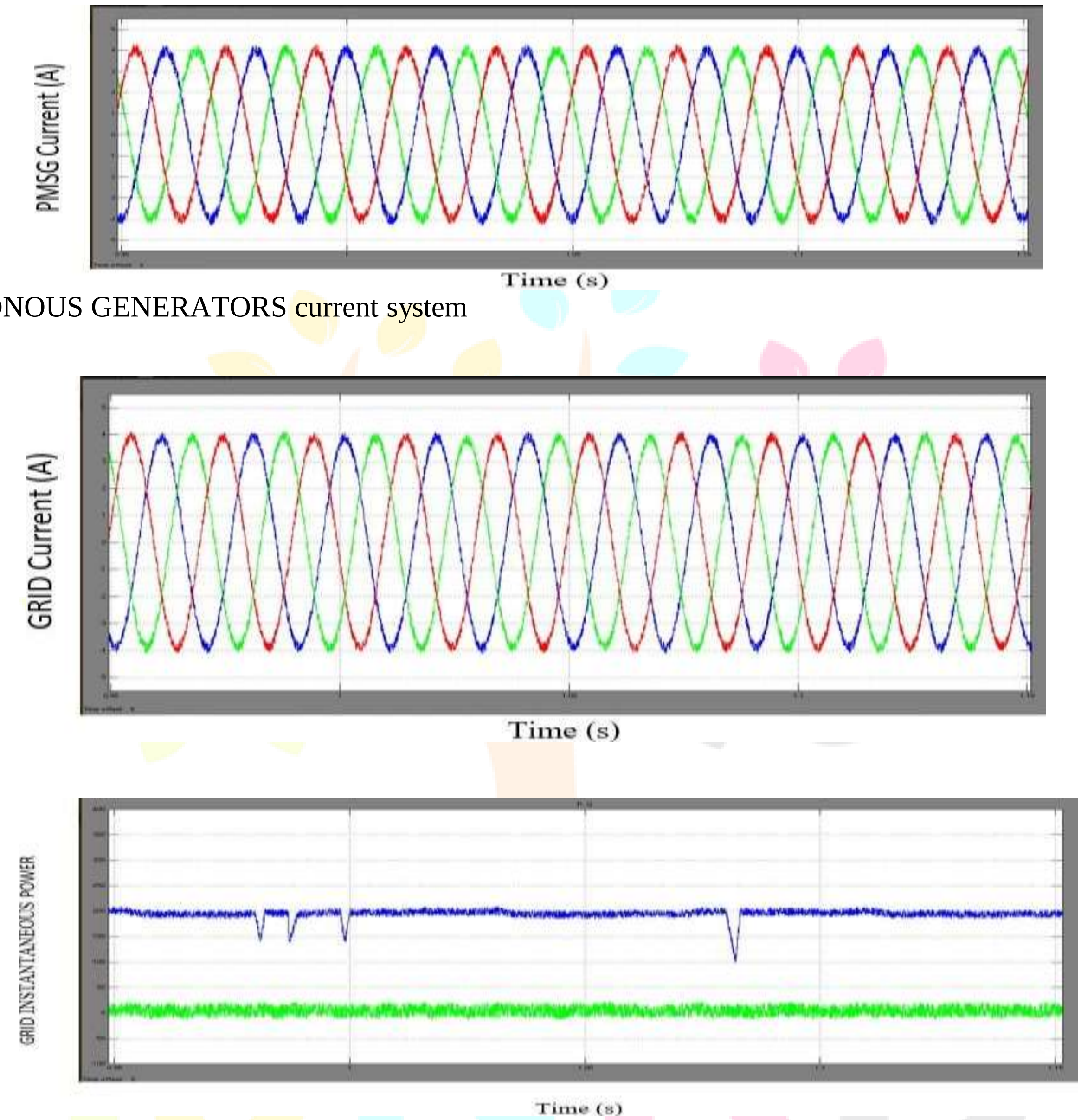

fig 7 simulation results of (a)PMSG current (b) grid current (c) grid instantaneous power

$$THD_{eq} = \sqrt{\frac{THD_A^2 + THD_B^2 + THD_C^2}{3}} \times 100\,\% \qquad (17)$$

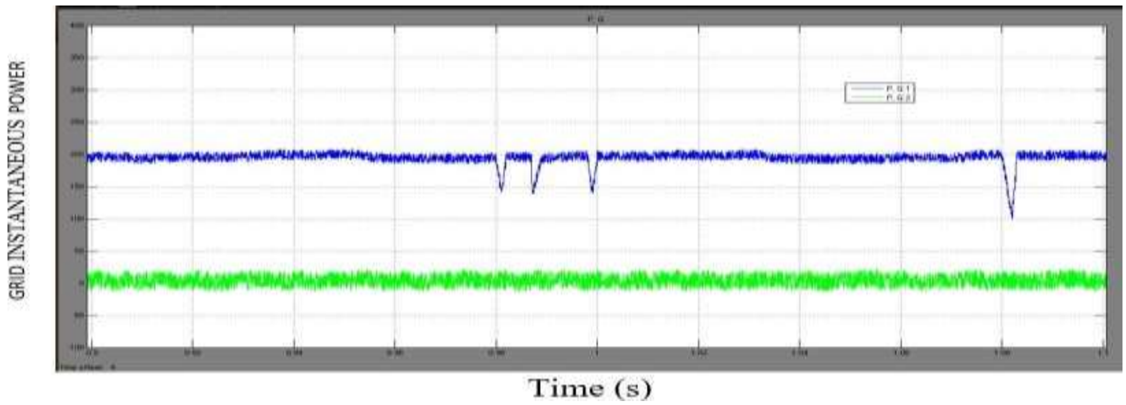
GRID INSTANTANEOUS POWER
Time (s)

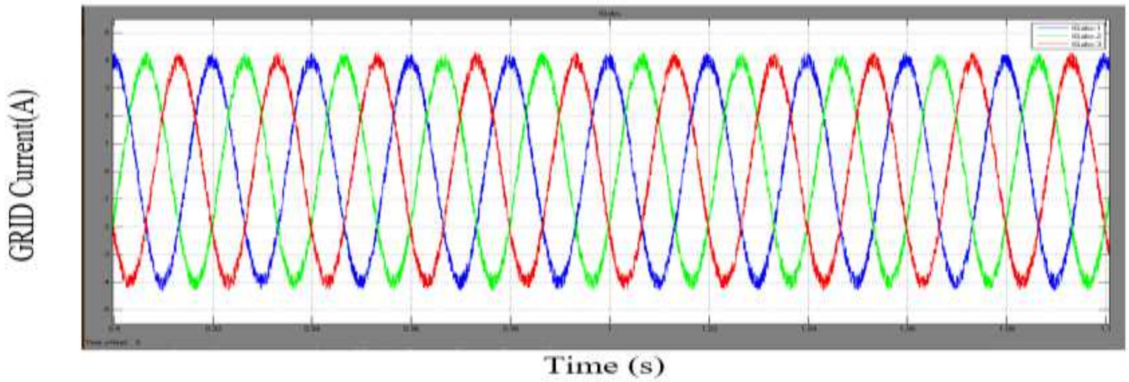
GRID Current(A)
Time (s)

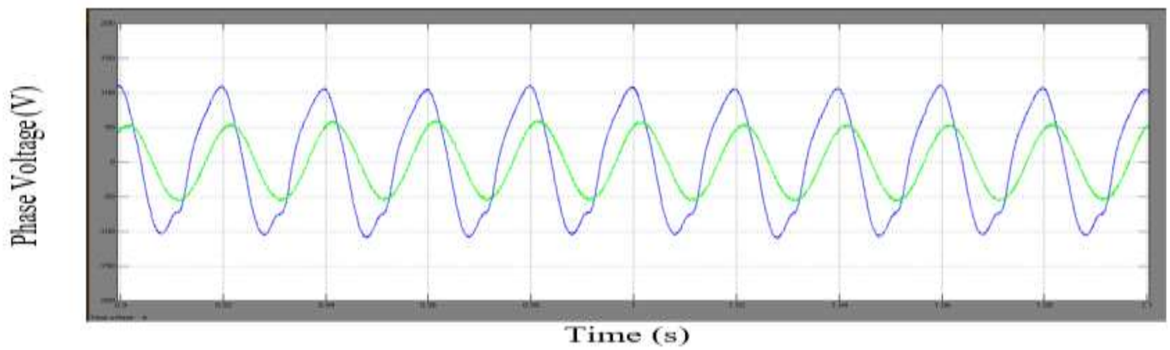
Phase Voltage (V)
Time (s)

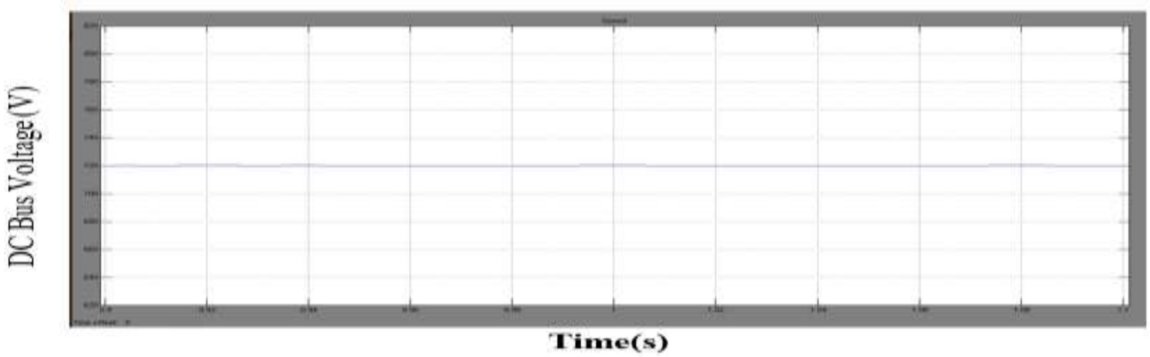
DC Bus Voltage (V)
Time(s)

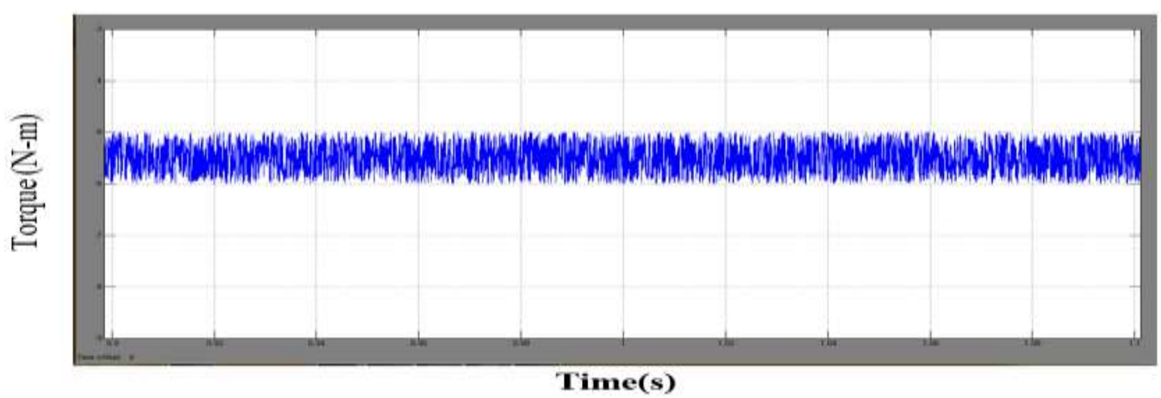
Torque (N-m)
Time(s)

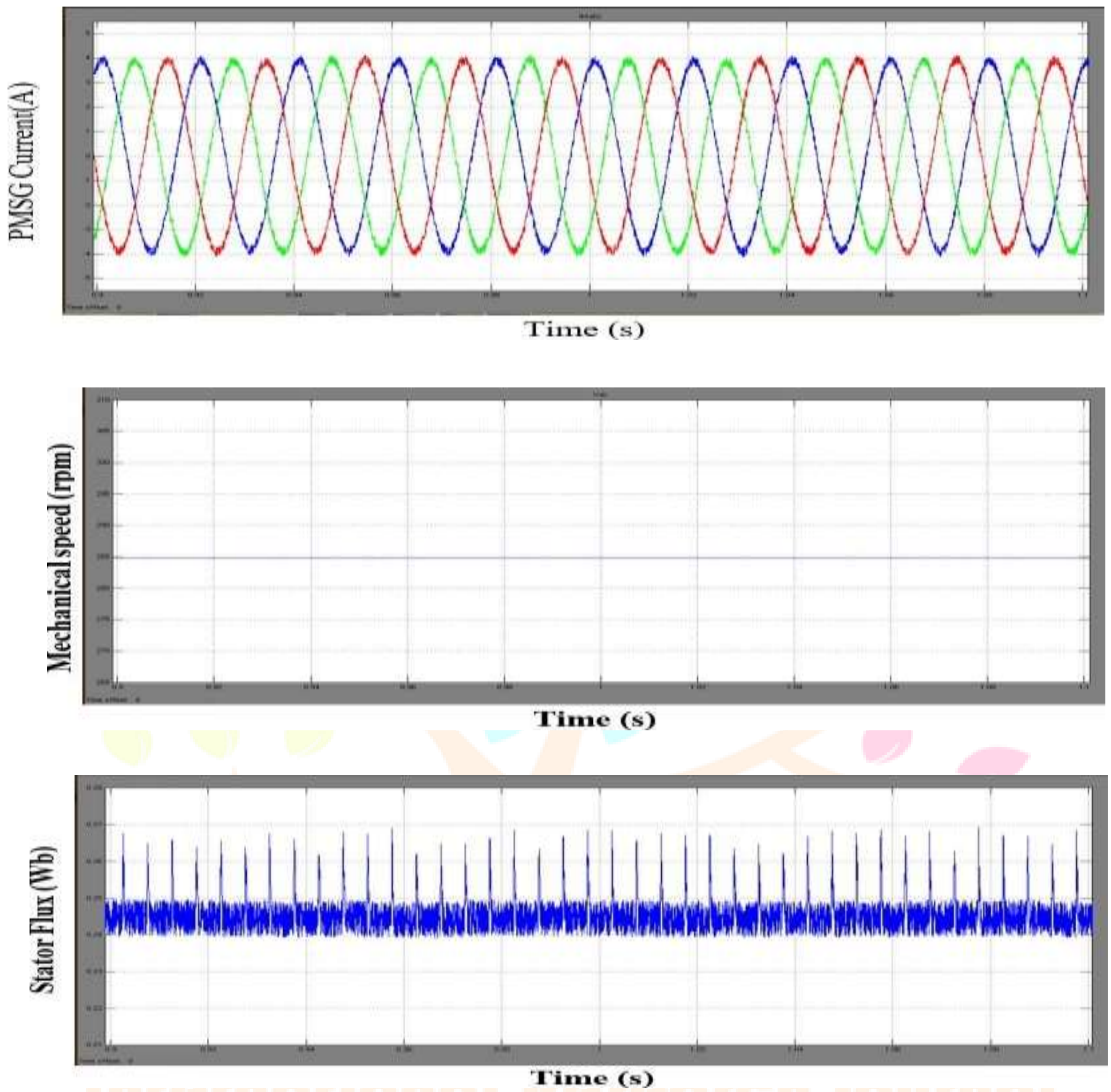

FIG. 8. WAVEFORMS OF OUTPUT (A) GRID INSTANTANEOUS POWER (B) GRID CURRENT (C) PHASE VOLTAGE (D) DIRECT CURRENT BUS VOLTAGE (E) TORQUE (F) PERMANENT MAGNET SYNCHRONOUS GENERATORS CURRENT (G) MECHANICAL SPEED (H) STATOR FLUX

$$TWO = \frac{\sqrt{X_{eRMS}^2 - X_{eDC}^2}}{|X_{eDC}|} \times 100\,\% \qquad (18)$$

Table VII demonstrates as the present Root Mean Square value is nearly equivalent for all 3∅, indicating that the system is operating in a well-adjusted manner, by way of vigorous method. Because

EMT and alternator ∅ currents were strongly connected, a slight drop in machine current THD results in a less oscillating electromagnetic torque waveform. As a result, when compared to the TWO value of 7.67 percent achieved in a healthy state, the TWO value below post fault operational situations drops for 7.64 percent. In same time, the suggested fault-tolerant control allows the machine to run with less flux TWO.

VII. CONCLUSIONS

After a power switch OPEN CIRCUIT fault occurs, a fault-tolerant direct-controlled PERMANENT MAGNET SYNCHRONOUS GENERATORS drive for wind turbine systems is suggested in this study, which maintains back-to-back converter procedure by suitable presentation. An instantaneous liability recognition system built on adaptive thresholds has implemented for this purpose, with the objective of swiftly diagnosing the defect and providing information for triggering appropriate corrective processes. To assure functioning within the area, a Five Leg Converter with Shared Leg is used to post fault procedure with back-to-back converters, and voltage capacity was raised through boosting the direct current bus voltage and reducing the alternator rpm. New direct control schemes have been devised to achieve independent control of the MS CONVERTER and GS CONVERTER by establishing new switching tables for the DTC, DPC approaches. As a result, active voltage vectors remain useful for the converters first, while both active and ZVV are applied to the other converter. As a consequence, as with the SLC are achieved. Controlling the instantaneous active and reactive powers, alternatively, achieves appropriate THD, UPF. As a result, all of the operating circumstances studied yield good results in ANFIS also.

References

[1] F. Spinato, P. J. Tavner, G. J. W. V. Bussel and E. Koutoulakos, "Reliability of wind turbine subassemblies," *IET Renew. Power Gener.*, vol. 3, no. 4, pp. 387–401, Dec. 2009.

[2] W. Qiao and D. Lu, "A survey on wind turbine condition monitoring and fault diagnosis-part I: components and subsystems," *IEEE Trans. Ind. Electron.*, vol. 62, no. 10, pp. 6536–6545, Oct. 2015.

[3] U. M. Choi, F. Blaabjerg, and K. B. Lee, "Study and handling methods of power igbt module failures in power electronic converter systems," *IEEE Trans. Power Electron.*, vol. 30, no. 5, pp. 2517–2533, May 2015.

[4] D. U. Campos-Delgado and D. R. Espinoza-Trejo, "An observer-based diagnosis scheme for single and simultaneous open-switch faults in induction motor drives", *IEEE Trans. Ind. Electron.*, vol. 58, no. 2, pp. 671-679, Feb. 2011.

[5] M. A. Rodríguez-Blanco, A. Claudio-Sánchez, D. Theilliol, L. G. Vela-Valdés, P. Sibaja-Terán, L. Hernández- González, J. Aguayo-Alquicira, "A failure-detection strategy for IGBT based on gate-voltage behavior applied to a motor drive system", *IEEE Trans. Ind. Electron.*, vol. 58, no. 5, pp. 1625-1633, May 2011

[6] N. M. A. Freire, J. O. Estima and A. J. M. Cardoso, "Open-circuit fault diagnosis in PMSG drives for wind turbine applications", *IEEE Trans. Ind. Electron.*, vol. 60, no. 9, pp. 3957-3967, Sep. 2013.

[7] N. M. A. Freire, J. O. Estima and A. J. M. Cardoso, "A voltage-based approach without extra hardware for

open- circuit fault diagnosis in closed-loop PWM AC regenerative drives", *IEEE Trans. Ind. Electron.*, Vol.61, no.9, pp.4960-4970, Mar. 2014.

[8] I. Jlassi, J. O. Estima, S. Khojet El Khil, N. Mrabet Bellaaj and A. J. M. Cardoso, "Multiple open-circuit faults diagnosis in back-to-back converters of PMSG drives for wind turbine systems," *IEEE Trans. Power Electron*., vol. 30, no. 5, pp. 2689-2702, May 2015.

[9] S. Khojet El Khil, I. Jlassi, J. O. Estima, N. Mrabet Bellaaj and A. J. M. Cardoso, "Current sensor fault detection and isolation method for PMSM drives, using average normalised currents," *IET Electronics Letters*, vol. 52, no. 17, pp. 1434-1436, Aug 2016.

[10] I. Jlassi, J. O. Estima, S. Khojet El Khil, N. Mrabet Bellaaj and A. J. M. Cardoso, "A Robust observer-based method for IGBTs and current sensors fault diagnosis in voltage-source inverters of PMSM drives," *IEEE Trans. Ind App*., vol. 53, no. 3, 2017.

[11] H. Yan, Y. Xu, F. Cai, H. Zhang, W. Zhao, and C. Gerada, "PWM-VSI Fault Diagnosis for PMSM Drive Based on Fuzzy Logic Approach", *IEEE Trans. Power Electron*., 2018 (*Early Access*)

[12] J. O. Estima and K. N. Gyftakis, "Voltage-source inverter-fed drives," in *Diagnosis and Fault Tolerance of Electric Machines, Power Electronics and Drives*, A. J. M. Cardoso (Editor), The Institution of Engineering and Technology, pp. 7-75, London, UK, (ISBN 978-1-78561-531-3), 2018.

[13] S. Karimi, A. Gaillard, P. Poure, and S. Saadate, "FPGA-based real time power converter failure diagnosis for wind energy conversion systems," *IEEE Trans. Ind. Electron*., vol. 55, no. 12, pp. 4299–4308, Dec. 2008.

[14] Z. Q. Zhu, K. Utaikaifa, K. Hoang, Y. Liu and D. Howe, "Direct torque control of three-phase PM brushless AC motor with one phase open-circuit fault," *IEEE International Electric Machines and Drives Conf.*, pp. 1180-1187, 2009.

[15] W. Sae-Kok, D. M. Grant, and B. W. Williams, "System reconfiguration under open-switch faults in a doubly fed induction machine," *IET Renew. Power Gener*., vol. 4, no. 5, pp. 458–470, Sep. 2010.